ARTICLE

Regulatory variants in *TCF7L2* are associated with thoracic aortic aneurysm

Tanmoy Roychowdhury,[1,27] Haocheng Lu,[1,27] Whitney E. Hornsby,[1] Bradley Crone,[2] Gao T. Wang,[3] Dong-chuan Guo,[4] Anoop K. Sendamarai,[5,6,7] Poornima Devineni,[5] Maoxuan Lin,[1,8] Wei Zhou,[1,9,10] Sarah E. Graham,[1] Brooke N. Wolford,[2] Ida Surakka,[1] Zhenguo Wang,[1] Lin Chang,[1] Jifeng Zhang,[1] Michael Mathis,[2,11] Chad M. Brummett,[11] Tori L. Melendez,[1] Michael J. Shea,[1] Karen Meekyong Kim,[12] G. Michael Deeb,[12] Himanshu J. Patel,[12] Jonathan Eliason,[13] Kim A. Eagle,[1] Bo Yang,[12] Santhi K. Ganesh,[1,14] Ben Brumpton,[15,16,17] Bjørn Olav Åsvold,[15,17,18] Anne Heidi Skogholt,[15] Kristian Hveem,[15,17] VA Million Veteran Program, Saiju Pyarajan,[5,7] Derek Klarin,[19,20,21] Philip S. Tsao,[22,23] Scott M. Damrauer,[24,25] Suzanne M. Leal,[3,26] Dianna M. Milewicz,[4] Y. Eugene Chen,[1,12] Minerva T. Garcia-Barrio,[1,*] and Cristen J. Willer[1,2,14,*]

Summary

Thoracic aortic aneurysm (TAA) is characterized by dilation of the aortic root or ascending/descending aorta. TAA is a heritable disease that can be potentially life threatening. While 10%–20% of TAA cases are caused by rare, pathogenic variants in single genes, the origin of the majority of TAA cases remains unknown. A previous study implicated common variants in *FBN1* with TAA disease risk. Here, we report a genome-wide scan of 1,351 TAA-affected individuals and 18,295 control individuals from the Cardiovascular Health Improvement Project and Michigan Genomics Initiative at the University of Michigan. We identified a genome-wide significant association with TAA for variants within the third intron of *TCF7L2* following replication with meta-analysis of four additional independent cohorts. Common variants in this locus are the strongest known genetic risk factor for type 2 diabetes. Although evidence indicates the presence of different causal variants for TAA and type 2 diabetes at this locus, we observed an opposite direction of effect. The genetic association for TAA colocalizes with an aortic eQTL of *TCF7L2*, suggesting a functional relationship. These analyses predict an association of higher expression of *TCF7L2* with TAA disease risk. *In vitro*, we show that upregulation of *TCF7L2* is associated with *BCL2* repression promoting vascular smooth muscle cell apoptosis, a key driver of TAA disease.

Introduction

Thoracic aortic aneurysm (TAA) is characterized by dilation of the aortic root, ascending aorta, the aortic arch, and descending aorta. TAA often develops asymptomatically over a period of time, and thus, early diagnosis of TAA is quite challenging. Aneurysms in thoracic aorta are frequently followed by rupture or dissection of aortic tissue, which can be fatal. Early diagnosis through selective screening of individuals with the highest genetic risk of TAA can potentially reduce the risk of death through early surgical intervention.[1]

Approximately 10%–20% of TAA cases are monogenic, i.e., due to rare, pathogenic variants in single genes.[2,3] Variants in at least 11 such genes (*ACTA2*, *COL3A1*, *FBN1*, *MYH11*, *SMAD3*, *TGFB2*, *TGFBR1*, *TGFBR2*, *MYLK*, *LOX*, and *PRKG1*) are associated with strong risk of TAA[4] and were primarily identified through family studies. Monogenic TAAs are often present with syndromic heritable thoracic aortic disorders, including Marfan, Loeys-Dietz,

Ehlers-Danlos, and smooth muscle dysfunction syndromes.[5,6] Moreover, approximately 50% of individuals with congenital heart malformations, such as bicuspid aortic valve (BAV), later develop TAA.[7] Yet the origin of the majority of TAA cases remains unknown. It is likely that these cases have more complex origins, involving common genetic variants affecting many genes. Genome-wide association studies (GWASs) have been particularly successful in identifying common genetic variants that increase disease risk. Previously, common variants in *FBN1* were found to be associated with TAA.[8] Another study implicated *LRP1* and *ULK4* in acute thoracic aortic dissection.[9]

In an attempt to identify genetic associations with TAA, we performed a GWAS of 1,351 TAA-affected individuals and 18,295 control individuals and identified a previously unpublished genome-wide significant locus in the third intron of *TCF7L2*. We replicated this signal with meta-analysis of four additional independent cohorts. At this locus, an inverse association between TAA and type 2 diabetes (T2D) was observed. The association signal colocalizes with an eQTL of *TCF7L2* in aorta, providing functional insight into the genetic association. *In vitro*, we show a potential role of *TCF7L2* in vascular smooth muscle cell (VSMC) apoptosis, a key TAA disease mechanism.

Material and methods

Description of the discovery cohorts

The Cardiovascular Health Improvement Project (CHIP) is a cohort with genotype data linked to electronic health records, family history, and aortic tissue from individuals seen at Michigan Medicine. The Michigan Genomics Initiative (MGI) is a hospital-based cohort with genotype data linked to electronic health records from individuals recruited during pre-surgical encounters at Michigan Medicine. Both studies were approved by the Institutional Review Board of the University of Michigan Medical School (IRBMED) (HUM00052866 and HUM00071298) and informed consent was obtained from study participants.

Genotype, QC, and imputation

CHIP and MGI samples were genotyped with two array versions of customized Illumina Infinium CoreExome-24 bead arrays: UM_HUNT_Biobank_11788091_A1 and UM_HUNT_Biobank_v1-1_20006200_A. A detailed description of these two arrays can be found in Fritsche et al.[10] Genotype calling was performed with Illumina GenomeStudio. Extensive quality control (QC) was performed prior to imputation. For CHIP samples, we first excluded samples with (1) rotated/swapped plates or DNA extraction batches, (2) duplicate/redundant samples with lower call rate, (3) identical ID and discordant genotypes or different ID but identical genotypes (both samples excluded), (4) gender discordance (unusual XY composition/no gender information available; no gender check possible/reported gender different from inferred sex), (5) large copy number variant, (6) estimated contamination $> 2.5\%$ (BAF Regress[11]), and (7) sample call rate $< 99\%$. In all samples, we excluded variants with (1) call rate $< 90\%$, (2) GenTrain score < 0.15, and (3) cluster separation < 0.3. After this, individual batches

in each array version were merged. We also obtained MGI samples with similar processing as described in Fritsche et al.[10] Next, from three sets (two CHIP array versions and MGI), we excluded samples with (1) outlier heterozygosity and (2) non-European ancestry as identified by laser[12] and variants with (1) call rate $< 99\%$ or (2) deviation from Hardy-Weinberg equilibrium (p value $< 10^{-4}$). Further analysis was restricted to variants present in both the MGI and two CHIP array versions among unrelated ($>3^{rd}$ degree) individuals identified via KING.[13] Variants with allele frequency differences between two array versions in CHIP (Chi-square; $p < 0.001$) were removed. Monomorphic variants were also excluded at this stage, generating 457,758 polymorphic variants from 42,119 samples after QC. As a preparation for imputation with the Haplotype Reference Consortium (HRC) panel,[14] we further excluded 71,942 variants from this set by using McCarthy group tools. The 385,816 variants that passed QC were used as input in the Michigan Imputation server. Imputation was performed with the HRC reference panel via Minimac4[15] with Rsq filter 0.3.

Case-control selection and association analysis

TAA-affected individuals were identified from both CHIP and MGI while control individuals were identified from MGI. Affected individuals in CHIP (n = 956) were defined as having an aneurysm in the thoracic aorta following diagnosis by cardiologists. Individuals with a known diagnosis of BAV were excluded because this is a strong risk factor of TAA, presumably because of altered haemodynamic blood flow and aortopathy instead of shared genetic architecture or molecular mechanisms.[16,17] Affected individuals in MGI (n = 395) were identified via International Classification of Diseases (ICD) codes (ICD9, 441.1/441.2; ICD10, I71.1/I71.2) excluding samples with a diagnosis of BAV (ICD9, 746.4; ICD10, Q23.1). After removing samples with any related diseases from the potential control individuals (phecodes 440–449.99), we used a case-control matching strategy to identify 18,295 control individuals from MGI (Table S1). We used R package MatchIt and applied nearest neighbor matching for birth year, PC1–4 (using Mahalanobis-metric matching), and exact matching for sex and array version. Association analysis was performed via SAIGE[18] with sex, birth year, array version, and PC1–4 as covariates. We reported results for all variants with minimum minor allele frequency (MAF) of 0.01 and minor allele count of 5.

Replication data and meta-analysis

The replication study from the University of Texas Health Science Center at Houston was approved by the institutional review board (IRB) (HSC-MS-01-251) and all subjects signed consent forms at recruitment to the study. The phenotyping and case-control association analysis is described in LeMaire et al.[8] Briefly, this data comprises 765 individuals of European ancestry with sporadic ascending aortic aneurysms or classic aortic dissection of the ascending or descending thoracic aorta (Stanford types A and B, respectively) and 875 control individuals. A logistic regression model was used for testing of variant association with the phenotype.

The VA Million Veteran Program (MVP) is comprised of veterans aged 18 to >100 years recruited from VA healthcare centers across the United States with genetic data linked to electronic health records. The study was approved by the VA central IRB and all participants provided informed consent. In MVP, 6,554 unrelated TAA-affected individuals of European ancestry were identified on the basis of the occurrence of a TAA ICD code (ICD9, 441.1/ 441.2; ICD10, I71.1/I71.2) on two distinct dates (individuals with BAV

were excluded; ICD9, 746.4; ICD10, Q23.1) and compared to 329,971 unrelated control individuals who were free of any codes listed in Table S2. Genotyping, imputation, and genomic quality control was performed as described elsewhere.[19] DNA variants were tested for their association with TAA via logistic regression in PLINK2 and controlled for age at time of analysis, age, gender, HARE ancestry assignment,[20] and the first five genetic principal components of ancestry (PCAs). Sensitivity analyses were then performed with participants who had undergone any form of thoracic aortic repair and subgroups of ascending and arch repair as cases based on Current Procedural Terminology (CPT) codes provided in Table S2. Covariates and controls were included in the same manner as the primary analysis.

The Trøndelag Health Study (the HUNT Study)[21] is a longitudinal population-based health survey conducted in Norway. Participation in the HUNT Study is based on informed consent, and the study has been approved by the Norwegian Data Protection Authority and the Regional Ethics Committee for Medical Research in Norway. Genotyping, quality control and imputation is described elsewhere.[22] We used ICD9 441.1/441.2 and ICD10 I71.1/I71.2 to identify 380 affected individuals and 69,255 control individuals from HUNT. Association analysis was performed via SAIGE[18] v.43.3 with sex, birth year, batch, and four PCs as covariates.

The UK Biobank[23] is a population-based cohort collected from multiple sites in the United Kingdom. We used ICD10 I71.1/I71.2 (excluding Q23.1) to identify 220 affected individuals among those of white British ancestry. After excluding samples with ICD10 I71.0–I71.9, 3,253 control individuals were selected by case-control matching as described in the discovery cohort. Association analysis was performed via SAIGE[18] with sex, birth year, array version, and four PCs as covariates.

Meta-analysis of three variants in the discovery and replication cohorts was performed by METAL[24] with the standard error approach.

Additional datasets

We downloaded the T2D GWAS in Europeans as "Mahajan.NatGenet2018b.T2D.European.gz" from the DIAGRAM consortium. The eQTL data in aorta as "Artery_Aorta.v8.signif_variant_gene_pairs.txt.gz" and "GTEx_v8_finemapping_CAVIAR.tar" were downloaded from the GTEx portal. DNase I hypersensitive site and H3K27ac of thoracic/ascending aorta (Table S3) were obtained from ENCODE. Promoter capture Hi-C data, as described in Jung et al.,[25] were obtained as "AO.po.txt.zip."

Conditional analysis

Approximate conditional analyses were performed with GCTA.[26] We used the –cojo-cond option to run conditional analyses with specific variants. We used the full summary statistics but limited the analysis to ± 500 kb of the conditional variant by using the –extract-region-snp parameter. For conditional analysis, imputed variants from CHIP+MGI (European ancestry) were used as the linkage disequilibrium (LD) reference. We reported the p value of rs7903146 in T2D GWAS conditional on rs4073288 and the p value of rs4073288 in TAA GWAS conditional on rs7903146 and other T2D variants (Table S4).

Colocalization

Colocalization analyses were performed with the R package coloc.[27] Coloc performs an approximate Bayes factor analysis with association statistics. We used the function coloc.abf() to calculate the posterior probabilities for the following: (H0) no association with either trait, (H1/H2) association with one of the two tested traits, (H3) association for both traits but different causal variants, and (H4) association for both traits with the same causal variant. A high posterior probability for H4 (PP4) indicates colocalization of the two trait associations. Variants in the ± 500 kb region surrounding rs4073288 were used for colocalization. The default prior probability for colocalization was used for both T2D and eQTL analyses.

Transcriptome-wide association study

To evaluate the evidence of colocalization between the TAA GWAS and eQTL association, we used the paradigm of transcriptome-wide association study (TWAS). TWAS methods perform gene-based association tests. We used these methods to test the association between gene expression predicted by cis-eQTLs and phenotype. We used the MetaXcan package[28] to run TWAS with TAA summary statistics. Briefly, we used GWAS tools from the MetaXcan package for summary statistics harmonization and imputation. The imputation step imputes missing GWAS variants via present GWAS variants and the GTEx genotypes. Next, we ran SPrediXcan with the imputed variants and the MASHR expression model (eQTL) of aorta from GTEx v.8.[29] We reported the Z scores and p values from this analysis. We did not observe any inflation of test statistics ($\lambda = 0.99$). No other genes except TCF7L2 had significant association after multiple testing correction for 13,951 genes present in the aortic expression model (p value significance threshold; $0.05/13,951 = 3.58 \times 10^{-6}$).

Fine-mapping

We employed FINEMAP,[30] a Bayesian fine-mapping method that implements a stochastic shotgun search algorithm incorporating the LD structure and associations (Z scores) in a locus, to identify potential causal variants. Variants with MAF > 5% in the ± 500 kb surrounding rs4073288 were used for this analysis. The LD structure in this locus was determined via PLINK[31] from imputed variants in CHIP/MGI. The fine-mapping was carried out with the assumption of a single causal variant. We constructed the 95% credible set by including the variants with highest posterior probabilities and until the sum of posterior probabilities was ≥0.95. We used RegulomeDB[32] to annotate variants. RegulomeDB uses public databases to aggregate information about eQTL, transcription factor binding/motif, DNase peak/footprint, etc. for each tested variant. The method assigns a rank to each variant that represents the likelihood of a variant's being a regulatory variant. We prioritized two variants by using this approach (Table S5). Because RegulomeDB operates in a tissue-agnostic manner, we checked the overlap of fine-mapped variants with the DNase I hypersensitive site and H3K27ac of thoracic/ascending aorta from ENCODE.[33] We configured custom tracks in UCSC genome browser to visualize the overlap of variant and chromatin marks. We obtained the promoter capture Hi-C in aorta from Jung et al.[25] The p values of chromatin interaction between promoter (chr10: 114,703,220–114,715,198) and variant (respective genomic bin) were reported.

LD score regression (LDSC)

We used "munge_sumstats.py" in LDSC[34] to format summary statistics. For further analyses, only variants with MAF > 0.01 and imputation Rsq > 0.9 and that were from Hapmap3 were incorporated. Heritability calculation was performed via the –h2 parameter (with –samp-prev and –pop-prev) in LDSC. Genetic correlations

between TAA and other traits were calculated in LD Hub.[35] Sources of summary statistics of these traits are listed in Table S6.

Adenoviruses

The Myc-tagged human full-length *TCF7L2* pcDNA3 plasmid was previously reported[36] (Addgene plasmid # 32738; RRID: Addgene_32738). The coding region of Myc-TCF7L2 from that plasmid was cloned into PCR8/GW/TOPO TA (entry) vector (K250020, Thermo Fisher Scientific) and recombined from the entry vector to the pAd/CMV/V5-DEST Vector (V49320, Thermo Fisher Scientific). The adenovirus carrying LacZ was described before.[37] The adenoviruses were packaged in HEK293A cells and purified by $CsCl_2$ density gradient ultracentrifugation. Adenovirus titration was determined by the Adeno-XTM quantitative PCR titration kit (Clontech, CA, USA).

Cell line growth and *TCF7L2* gain and loss of function *in vitro*

Primary human aortic smooth muscle cells (HASMCs) (Lonza, CC2571, lot # 000335663, Walkersville, MD, USA) were grown in smooth muscle cell growth medium 2 containing 5% fetal bovine serum (PromoCell, Germany) and 1% penicillin/streptomycin solution (GIBCO, #15140122) at 37°C with 5% CO_2 in a humidified incubator and subjected to quiescence in Opti-MEM for 48 h when so required. HASMCs were used from passage 5 to 8. For overexpression of *TCF7L2*, adenoviruses containing myc-tagged *TCF7L2* or LacZ (control) under the control of the cytomegalovirus (CMV) promoter were used for infection at 30 MOI. For knockdown, cells were transfected with siRNA against *TCF7L2* (Horizon D-003816-01 sequence: GAUGGAAGCUUACUAGAUU) or siRNA control (Horizon D-001206-14) at a concentration of 30 nM with Lipofectamine RNAiMAX for 72 h in serum-free medium (Opti-MEM) before use for apoptosis studies.

Apoptosis studies

HASMCs with gain or loss of TCF7L2 as above were treated with 100 ng/mL Fas ligand (FasL) (Enzo Life Science: ALX-522-020) for the indicated times in Opti-MEM, as we previously reported[37] (48 h after adenoviral infection or 72 h after siRNA treatment). For annexin V studies, cells were treated for 4 h with FasL in Opti-MEM medium (31985062, GIBCO). Cells were dissociated with 0.25% trypsin (25200056, GIBCO) and stained with the FITC Annexin V Apoptosis Detection Kit I (556548, BD Biosciences), as we previously reported.[37] In brief, the cells were washed with cold PBS twice, suspended in 1× binding buffer and stained with FITC annexin V and propidium iodide (PI). The flow cytometry analysis was performed by the flow cytometry core at the University of Michigan with a MoFlo Astrios Cell Sorter (Beckman Coulter, Brea, CA). Apoptotic cells are defined as FITC annexin V positive and PI negative. For immunoblot, cells were treated for 6 h with FasL and subjected to immunoblot with standard protocols as described below.

Quantitative real-time PCR and immunoblot

HASMCs were grown and treated as indicated in each case. For quantitative real-time PCR, we isolated total RNA from HASMCs with the RNeasy Mini Kit (QIAGEN, #74106) followed by the SuperScript III First-Strand Synthesis System (Invitrogen, #18080051) by using random hexamers to generate cDNA, as suggested by the respective manufacturers. Gene expression was quantified in triplicates by quantitative real-time PCR with IQ SYBR Green Supermix (Bio-Rad, #1708882). Relative levels were determined via the ΔΔCt

method with expression of the *ACTB* (Actin Beta) gene as the internal control. The qPCR primer sequences are listed in Table S7. For immunoblot, cell extracts were prepared with RIPA lysis buffer supplemented with complete EDTA-free protease inhibitor cocktail (Roche, #11836170001, Penzberg, Germany) and PhosSTOP phosphatase inhibitor (Roche, #4906845001). The protein concentration was determined with the Bradford assay (Bio-Rad, #5000002) and a GloMax Explorer Multimode Microplate Reader. A total of 40 μg of total protein/lane was resolved in SDS-PAGE gels (Bio-Rad 4561094) and transferred to nitrocellulose membranes (Bio-Rad, #1620115, Hercules, CA) with standard techniques. Antibodies were used as follows: the BCL2 antibody (ab182858, 1.2 μg/mL) from Abcam (UK); β-actin (#3700, 0.65 μg/mL), PARP (#9542, 0.1 μg/mL), Caspase 3 (#9662, 0.05 μg/mL), cleaved Caspase 3 (#9664, 0.04 μg/mL), BAX (#5023, 0.14 μg/mL), and myc (#2276, 0.3 μg/mL) from Cell Signaling Technology (CST, Danvers, MA); and the secondary antibodies, IRDye 800CW Donkey anti-Rabbit IgG and IRDye 680RD Donkey anti-Mouse IgG at 0.2 μg/mL, from LI-COR Bioscience (Lincoln, NE). We collected data by using the Odyssey CLx Imaging System (LI-COR Bioscience) and quantified data with the LI-COR Image Studio Software to determine the protein abundance relative to β-actin.

Results

We performed genetic discovery association analysis of 1,351 affected individuals and 18,295 control individuals (European ancestry) from the Cardiovascular Health Improvement Project (CHIP) and Michigan Genomics Initiative (MGI) at the University of Michigan, Michigan Medicine. Imputation with the HRC panel in the Michigan Imputation Server enabled testing of 22.9 million variants. We did not observe any evidence of inflation ($\lambda_{GC} = 1.04$) of the association test statistics (Figure S1A). Using LD score regression with sample- and population-level prevalence (6% and 0.34%,[38] respectively), we estimated SNP heritability of TAA as 0.11 (SE = 0.04) in liability scale. Next, genetic correlation between TAA and known risk factors was examined with GWAS summary statistics (Table S6). We observed a positive genetic correlation between TAA and height ($r_g = 0.32$, SE = 0.11, p = 0.003). This correlation remained significant after excluding variants within 500 kb from rs591519 (*FBN1*, a gene associated with Marfan syndrome and related disorders) from TAA summary statistics. We did not observe a significant genetic correlation between TAA and smoking or lipid traits, two factors strongly correlated with abdominal aortic aneurysm (AAA).[39] On the contrary, diastolic blood pressure is positively correlated with TAA ($r_g = 0.27$, SE = 0.09, p = 0.003) but systolic blood pressure is not ($r_g = -0.006$, SE = 0.08, p = 0.93).

Association with TAA at the *TCF7L2* locus

57 variants from two loci reached genome-wide significance ($p < 5 \times 10^{-8}$) in our analysis (Figure S1B). First, we replicated a significant association at the previously known *FBN1* locus (index variant rs591519, A/T, effect allele: T, β = 0.42, SE = 0.06, OR 95% CI = 1.35–1.71,
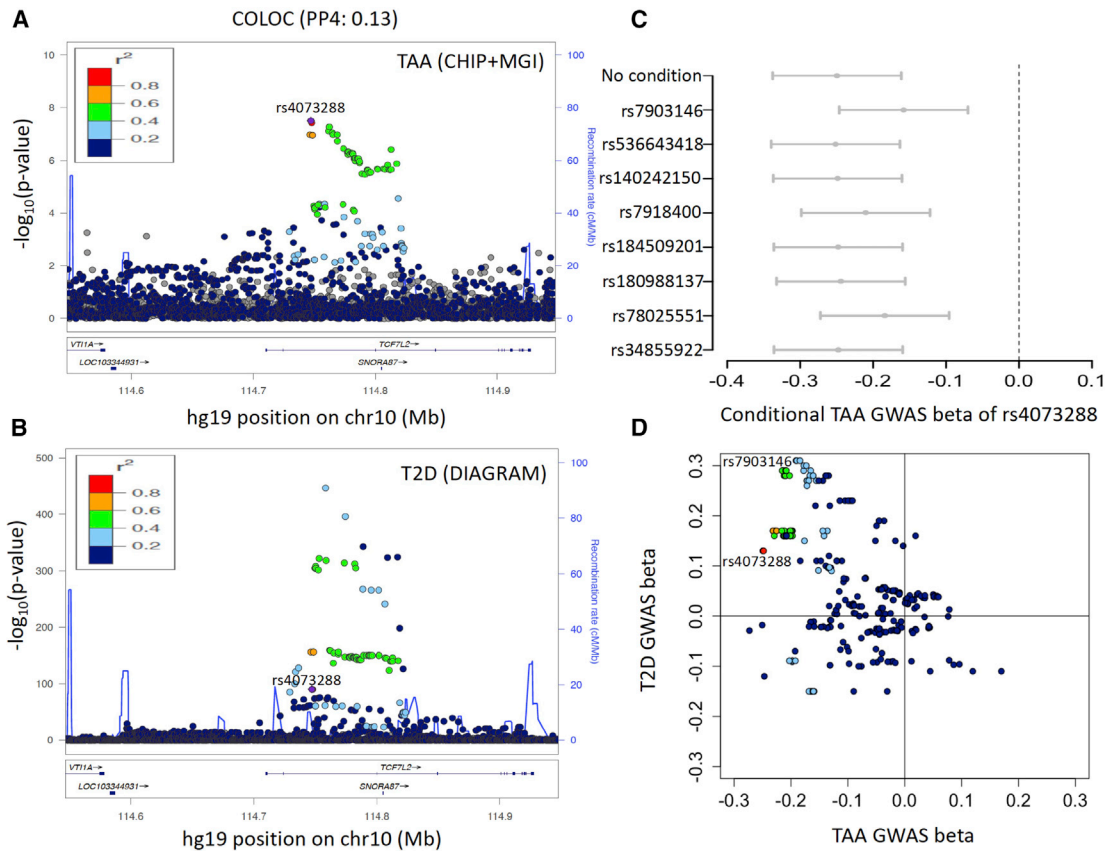
Figure 1. _TCF7L2_ locus in TAA and T2D

(A) LocusZoom plot of _TCF7L2_ locus in TAA GWAS from CHIP+MGI.
(B) LocusZoom plot of _TCF7L2_ locus in T2D GWAS from DIAGRAM. LD colors are with respect to the TAA index variant rs4073288.
(C) Conditional effect sizes (beta, in SD units) of TAA index variant rs4073288 in TAA GWAS. Eight independent T2D variants were used for conditioning. Error bars represent 95% confidence intervals.
(D) Comparison of effect sizes (beta) in TAA and T2D GWAS. Variants in this locus have opposite direction in effect sizes in TAA versus T2D GWAS.

$p = 1.1 \times 10^{-9}$). Second, we identified a previously unpublished TAA association in the intronic region of _TCF7L2_ in chromosome 10 (Figure 1A). The index variant rs4073288 (Table 1) is a common variant with an MAF of 0.32 in cases and 0.37 in controls. We observed 49 common variants (MAF range: 0.37–0.47) with $p < 5 \times 10^{-6}$ in this locus (three genotyped; 46 imputed, Rsq: 0.88 to 0.94). A conditional analysis on rs4073288 did not identify any secondary independent variants in this locus. At both the _TCF7L2_ and _FBN1_ loci, we observed a reduced effect in MGI compared to CHIP cases (Table S8). Among 956 CHIP cases, approximately 80% and 8% were classified as ascending and descending TAA, respectively. Interestingly, at the _TCF7L2_ locus, we observed stronger effect in descending TAA, while the _FBN1_ effects were stronger in ascending TAA (Table S8). We observed lower effects in the same direction for association with AAA[39] at _TCF7L2_ (rs4073288, effect allele: A, β = −0.05, SE = 0.02, OR 95% CI = 0.91–0.99, $p = 3.1 \times 10^{-3}$) as well as _FBN1_ (rs591519, effect allele: T, β = 0.06, SE = 0.03, OR 95% CI = 1–1.13, p = 0.03). These variants were not significant (p > 0.05) for association with intracranial aneurysm.[40]

Next, we sought replication of the _TCF7L2_ locus in a meta-analysis of four independent datasets of European ancestry from (1) University of Texas Health Science Center at Houston (UT, 765 affected individuals), (2) The Trøndelag Health Study (the HUNT Study, 380 affected individuals), (3) UK Biobank (220 affected individuals), and (4) the Million Veteran Program (MVP, 6,554 affected individuals). We observed consistent direction of effect sizes in all replication cohorts (Figure S2). At both the _TCF7L2_ and _FBN1_ loci, substantial differences in effect estimates among cohorts were observed (Figure S2). _TCF7L2_ effect estimates were similar between the Michigan discovery and UT datasets, two cohorts that were primarily ascertained from aortic clinics, whereas the other datasets used ICD-based phenotypes from large biobanks. In MVP, we further identified a smaller subset of TAA-affected individuals in whom surgical repair was performed (730 affected individuals). We observed stronger effect estimates in these affected individuals compared to ICD-based phenotypes (three _TCF7L2_ variants, OR = 0.86–0.89 for surgical repair TAA versus OR = 0.94 for all ICD-derived TAA-affected individuals; Table S9). This observation highlights the

Table 1. Discovery and replication of *TCF7L2* variants in TAA

Variant	EA	OA	Discovery				Replication				Discovery + replication			
			Beta	SE	OR 95% CI	p	Beta	SE	OR 95% CI	p	Beta	SE	OR 95% CI	p
rs4073288 (index)	A	G	−0.25	0.04	0.72–0.84	3.1×10^{-8}	−0.07	0.02	0.90–0.97	4.2×10^{-5}	−0.10	0.02	0.87–0.94	5.2×10^{-9}
rs7904519 (genotyped)	G	A	−0.21	0.04	0.75–0.88	3.6×10^{-7}	−0.07	0.02	0.90–0.97	1.7×10^{-5}	−0.09	0.01	0.90–0.93	3.3×10^{-9}
rs4074718 (fine-mapped)	A	G	−0.23	0.04	0.73–0.86	1.1×10^{-7}	−0.07	0.02	0.90–0.97	4.0×10^{-5}	−0.09	0.02	0.88–0.95	5.8×10^{-9}

EA, effect allele; OA, other allele.

limitation of replication with cohorts with different phenotype definitions and/or case-ascertainment strategies. Nonetheless, after combining all replication datasets, we observed an association p value $< 5 \times 10^{-5}$ for all three tested variants at *TCF7L2* (Table 1).

Comparison of the *TCF7L2* association with TAA and type 2 diabetes

TCF7L2 is known to be associated with T2D.[41] A common variant in the 3rd intron of *TCF7L2* is associated with T2D and most likely causes a defect in insulin secretion in the pancreas.[42] The TAA index variant rs4073288 is in relatively low LD with the T2D index variant rs7903146 ($R^2 = 0.28$ in Europeans, ~11 kb apart, 3rd intron). We further examined GWAS summary statistics of T2D from Mahajan et al.[43] (rs7903146, $P_{T2D} = 1.5 \times 10^{-447}$; rs4073288, $P_{T2D} = 3.8 \times 10^{-91}$) (Figure 1B). Although the same region within *TCF7L2* (3rd intron) is associated with both TAA and T2D risk, the posterior probabilities from colocalization analysis indicated independent signals for TAA and T2D (COLOC, PP3 = 0.85, PP4 = 0.13). Also, a reciprocal conditional analysis did not diminish either signal completely (TAA, $P_{cond:rs7903146}$ rs4073288 = 4.5×10^{-4}; T2D, $P_{cond:rs4073288}$ rs7903146 = 3.4×10^{-262}). Mahajan et al. reported seven other secondary independent variants associated with T2D in this locus, which may be functional in different tissues.[43] All of these secondary T2D variants have very low correlation with the TAA index variant rs4073288 (maximum $R^2 = 0.24$; Table S4). The association between rs4073288 and TAA remained significant when we conditioned on each of these eight T2D variants (Figure 1C). These observations suggest the presence of different causal variants for TAA and T2D. Finally, we noted an opposite direction of effect (Figure 1D) for TAA and T2D at variants in this region (rs4073288, effect allele: A, β_{TAA} = −0.24 [0.04], β_{T2D} = 0.13 [0.006]; rs7903146, effect allele: T, β_{TAA} = −0.18 [0.04], β_{T2D} = 0.31 [0.006]). The opposite direction of effect for T2D and TAA was consistent in all variants with $P_{TAA} < 5 \times 10^{-6}$ in this locus. We did not observe a significant genetic correlation between TAA and T2D (r_g = 0.006, SE = 0.15, p = 0.96) via GWAS summary statistics.

Higher expression of *TCF7L2* in aorta is associated with TAA risk

To investigate a potential effect of TAA GWAS variants on expression of *TCF7L2*, we looked for tissue-specific cis-eQTLs from GTEx v.8.[29] The TAA index variant rs4073288 is an eQTL of *TCF7L2* in aorta (effect allele: A, normalized effect size = −0.27, p = 2.6×10^{-11}, N = 387). The TAA risk allele (G in rs4073288) is associated with higher expression of *TCF7L2* in aorta (Figure S3A). This eQTL association was not observed in any other tissue (Figure S3B). Further analysis revealed colocalization (Figure 2B) between the GWAS and eQTL signal (COLOC, PP3 = 0.03, PP4 = 0.96). Next, we performed a TWAS analysis by using SPrediXcan[28] with the MASHR aortic expression model from GTEx v.8. This resulted in a significant association between predicted expression levels of *TCF7L2* and TAA (Z score = 5.35; p = 8.38×10^{-8}; Bonferroni corrected threshold: 0.05/13,951 = 3.58×10^{-6}; Figure S3C). A positive Z score in TWAS indicated that higher expression of *TCF7L2* is associated with TAA disease. This observation suggests a probable disease mechanism of TAA-associated variants via an increase of *TCF7L2* expression in aorta.

Investigation of the causal variant in the *TCF7L2* locus

We hypothesize that the TAA causal variant affects the expression of *TCF7L2* via alteration of some regulatory element in this region. In an attempt to identify the causal variant, we applied a Bayesian fine-mapping approach, FI-NEMAP.[30] The 95% credible set for the GWAS consisted of 32 variants from this locus. We also obtained the fine-mapped variants in eQTL by CAVIAR[44] from GTEx. Out of 32 variants in the GWAS credible set, 23 were also present in the 95% causal set of eQTL (Figure S4A). Next, we used RegulomeDB[32] to annotate variants with known or predicted regulatory elements. We could further prioritize (Table S5) two variants in the common credible set (Figure 2B). Both these variants (rs4074718 and rs4077527) have larger effect sizes for the *TCF7L2* eQTL than the index variant rs4073288. While both variants are from regions annotated as enhancers in multiple tissues, rs4077527 intersects with accessible chromatin (DNase I hypersensitive site) in adult thoracic/ascending aorta in ENCODE[33] data (Figure 2C, Table S3). We also observed strong evidence of enhancer activity (H3K27ac) in these samples overlapping rs4077527. Because both these variants are quite far from the *TCF7L2* promoter (rs4074718, ~40 kb; rs4077527, ~10 0kb), we examined promoter capture Hi-C data from aorta.[25] A significant long-distance chromatin interaction (p < 0.01, as per methods in Jung et al.[25])
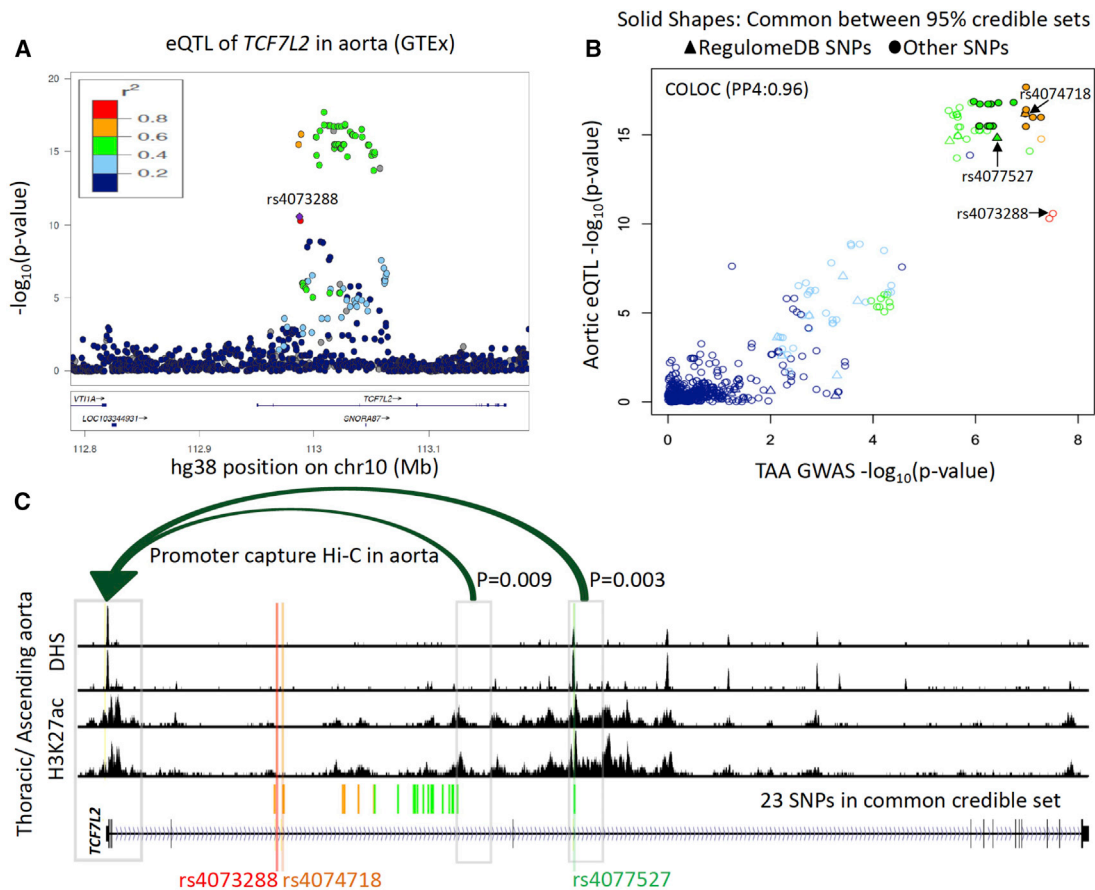
Figure 2. Functional characterization of *TCF7L2* locus
(A) LocusZoom plot of aortic eQTL of *TCF7L2*. LD colors are with respect to the TAA index variant rs4073288.
(B) Comparison of p values in TAA GWAS and aortic eQTL from GTEx. These two associations colocalize with posterior probability 0.96 by COLOC. The solid shapes represent 23 variants that were in both GWAS and eQTL 95% credible sets. Two variants were prioritized by RegulomeDB (rs4074718 and rs4077527).
(C) Regulatory landscape of *TCF7L2* gene body in thoracic aorta/ascending aorta from ENCODE. The fine-mapped variant rs4077527 intersects with DNase I hypersensitive site (DHS) and H3K27ac in this tissue. Using promoter capture Hi-C in aorta, we highlighted only genomic bins that significantly interact (p < 0.01) with *TCF7L2* promoter. Promoter capture Hi-C p values for 23 variants are given in Figure S4B.

between rs4077527 and the *TCF7L2* promoter region (hg19; chr10: 114,703,220–114,715,198) was observed (Figure 2C, Figure S4B). Together, these observations predict rs4077527 as a strong candidate for the causal TAA variant in this locus, most likely interacting with the promoter to impact *TCF7L2* expression in the aorta.

TCF7L2 enhances human vascular smooth muscle cell apoptosis

TAA is characterized by vascular smooth muscle cell (VSMC) apoptosis in association with loss of their contractile phenotype, inflammatory status, and increased extracellular matrix degradation as drivers of adverse outcomes.[45] Loss of VSMC in TAA is recognized to be the result of increased apoptosis through the endogenous pathway regulated via *BCL2*.[45,46] As a distal effector of the Wnt/β-catenin/TCF-LEF pathway, *TCF7L2* is known to regulate homeostasis of VSMC, the media layer of blood vessels, including phenotypic modulation and proliferation.[47–49] *TCF7L2* may exert pro-[50,51] or anti-apoptotic[52,53] effects

in different contexts. Yet, contribution of *TCF7L2* to VSMC apoptosis in aneurysm remains unaddressed. We experimentally assessed whether gain and loss of function of *TCF7L2* contributes to VSMC apoptosis via differential regulation of *BCL2* expression in human aortic smooth muscle cells (HASMCs) *in vitro*. Adenoviral-mediated overexpression of *TCF7L2* resulted in reduced *BCL2* expression of both mRNA (54% reduction, p = 0.0004) and protein (24% reduction, p = 0.0011) (Figures 3A and 3B, Figure S5A) compared with the adenoviral-mediated expression of LacZ used as control. Conversely, siRNA-mediated downregulation of *TCF7L2,* which resulted in a significant reduction in endogenous *TCF7L2* mRNA (80% reduction, p = 0.0002 versus siRNA control) and protein (77% reduction, p = 0.0145 versus siRNA control), demonstrated a concomitant increase in *BCL2* protein (1.6-fold increase, p = 0.0154 versus shRNA control) and mRNA abundance (2.7-fold increase, p = 0.0001) (Figures 3C and 3D, Figure S5B). Changes in *TCF7L2* showed no significant effects on BAX protein or mRNA expression (Figures 3A–3D,
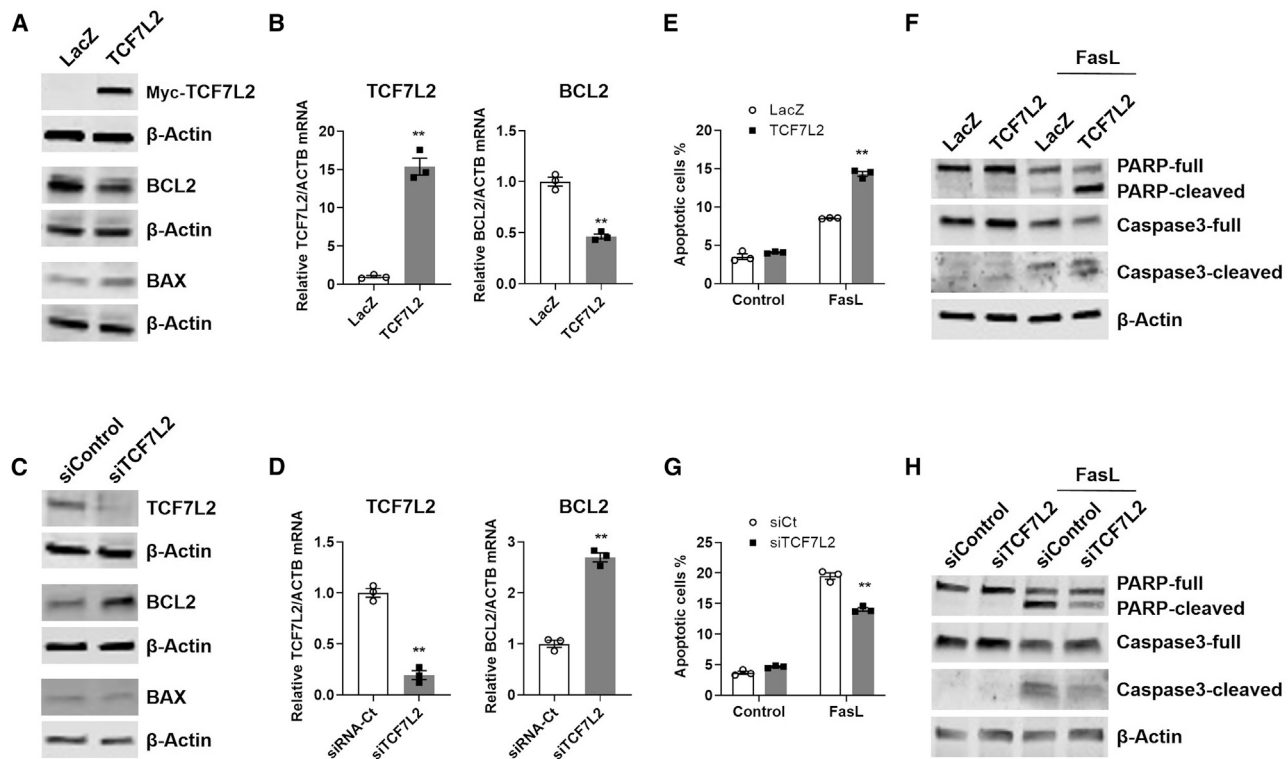
Figure 3. _TCF7L2_ expression is directly associated with vascular smooth muscle cell apoptosis _in vitro_
HASMCs were infected with adenovirus (30 MOI)-encoding LacZ (control) or myc-tagged _TCF7L2_, and after 48 h, (A) the abundance of the indicated proteins in the cell extracts was determined by immunoblot (representative of three independent experiments) and (B) the mRNA expression of the indicated genes, relative to ACTB, by quantitative real-time PCR. A LacZ control was set at 1 as reference (n = 3; representative of three independent experiments). Data are mean ± SEM. **p ≤ 0.0004. HASMCs were transfected with siRNA control or siRNA against _TCF7L2_ via Lipofectamine RNAiMax, and after 72 h, (C) the abundance of the indicated proteins and (D) the mRNA expression of the indicated genes were determined as described above with an siRNA control set at 1 as reference. **p ≤ 0.0002. HASMCs were infected with adenovirus as in (A). After 48 h in serum-free medium, they were treated with Fas ligand (FasL, 100 ng/mL) in serum-free medium and apoptosis was assessed by (E) annexin V via FACS analysis after treatment for 4 h (n = 3; representative of three independent experiments) or (F) the abundance of the indicated proteins in the cell extracts after 6 h as determined by immunoblot (representative of three independent experiments). HASMCs were transfected with the indicated siRNA as in (C). After 72 h in serum-free medium, they were treated with FasL (100 ng/mL) for (G) annexin V assay after 4 h as in (E) or (H) immunoblot after 6 h as in (F) and subjected to immunoblot as in (E). Densitometry for (A), (B), (E), (F), and mRNA expression of _BAX_ are provided in Figure S5.

Figures S5A–S5D). Consequently, we determined a significant BAX/BCL2 protein ratio between _TCF7L2_ overexpression and knockdown (1.3222 ± 0.1024 versus 0.6426 ± 0.1176, p = 0.0168, respectively) in basal growth conditions (Figures 3A and 3B, Figure S5A), suggesting a potential pro-apoptotic effect of _TCF7L2_ upregulation in HASMCs.

We further examined the expectation that increased _TCF7L2_ expression enhances apoptosis of aortic smooth muscle cells through treatment with FasL, a potent inducer of VSMC apoptosis produced by inflammatory cells in the aneurysmal tissues.[45,54] In these experimental conditions, FasL treatment resulted in significant increase in annexin V positive cells (1.7-fold, p ≤ 0.0001), indicative of enhanced early apoptosis when _TCF7L2_ was overexpressed (Figure 3E, Figure S5E), while siRNA-mediated _TCF7L2_ knockdown significantly reduced the apoptotic response by 28% (p ≤ 0.0001) (Figure 3G, Figure S5F), as determined by fluorescence-activated cell sorting (FACS). These data were in agreement with progression into apoptosis upon _TCF7L2_ overexpression, as indicated by significantly

increased cleavage of PARP and caspase-3 compared to the corresponding full-length proteins (Figure 3F, Figure S5G). Conversely, siRNA-mediated knockdown of _TCF7L2_ significantly reduced cleavage of both apoptosis markers (Figure 3H, Figure S5H). Overall, these data indicate that increased expression of _TCF7L2_ may result in enhanced apoptosis of vascular smooth muscle cells—a likely mechanism of action of TAA-associated variants in _TCF7L2_.

Discussion

In this study, we identified a locus in the intronic region of _TCF7L2_ that is associated with TAA, to our knowledge, the first locus identified for TAA via genome-wide approaches. Using eQTL from aorta, we provide evidence that TAA-associated variants are associated with altered expression of _TCF7L2_ and we highlight one variant in the locus that overlaps with an enhancer active in aorta. Common variants (rs7903146, index variant) in this locus are

the strongest known genetic risk factor for T2D.[42] Vinuela et al.[55] demonstrated that the T2D risk allele of rs7903146 decreases pancreatic islet expression of the last (3′) exon of *TCF7L2*. Although there is evidence of different causal variants for TAA and T2D, we observed an opposite direction in effect sizes. Interestingly, epidemiological studies have historically suggested an inverse relationship between aortic aneurysm and T2D.[56–58] Our genetic results suggest that, at least for the *TCF7L2* locus, shared but independent etiology (gene-level horizontal pleiotropy) may be partially responsible for this association. These results most likely indicate that largely independent sets of causal variants lead to increased *TCF7L2* expression in the human aorta and decreased *TCF7L2* expression in pancreatic islets.

The T-cell factor/lymphoid enhancer factor (TCF/LEF) transcription factors (including *TCF7L2*) are signal integrators and effectors of the Wnt/β-catenin pathway with contextual tissue and cell-type-specific functions[59] and can exhibit differential effects because of epigenetic modifications of the target genes. Wnt/β-catenin is an evolutionarily conserved pathway that regulates various aspects of development, including cell proliferation, migration, polarity, and apoptosis.[60] Dysregulation of the Wnt/β-catenin signaling is involved in a wide range of disorders, including Alzheimer disease, cancer, and metabolic diseases.[61] Current research supports a role of *TCF7L2* in vascular development.[62–64] In cardiovascular diseases, the Wnt/β-catenin pathway was found to be dysregulated in restenosis,[65] and more recently, *TCF7L2* was demonstrated to regulate VSMC plasticity in both *GATA6*-dependent and -independent fashions.[47] Regarding aneurysm, Krishna et al. reported activation of the Wnt/β-catenin pathway in AAA via epigenetic silencing of the Wnt inhibitor sclerostin.[66] Recently, dysregulated Notch/BMP/WNT pathways were found in aortic endothelial cells isolated from individuals with TAA compared to healthy donors,[67] including increased *TCF7L2* mRNA expression and activation of the Wnt/β-catenin pathway in the endothelium. Our analyses indicate that variants associated with higher expression of *TCF7L2* are also associated with TAA. TAA is a disease characterized by VSMC death as a driver of adverse outcomes.[45] Therefore, we specifically addressed the potential effects of *TCF7L2* on VSMC apoptosis *in vitro*. We show that *TCF7L2* expression is directly associated with VSMC apoptosis and that this effect could be mediated, at least in part, through *TCF7L2* repression of *BCL2* expression, a known target of the pathway. Our data from VSMC, together with the report from endothelial cells,[67] clearly indicate that upregulation of *TCF7L2* may play a fundamental role in TAA pathology.

Mendelian, monogenic inheritance of TAA is primarily driven by pathogenic variants in genes from the TGF-β signaling pathway (*FBN1*, *SMAD3*, *TGFB2*, *TGFBR1*, and *TGFBR2*) and VSMC contraction pathway (*ACTA2*, *MYH11*, *MYLK*, and *PRKG1*). The TGF-β/*SMAD*3 pathway interacts with β-catenin in the canonical Wnt/β-catenin signaling pathway toward activation of TCF/LEF transcription factors (including *TCF7L2*) (Figure S6). Future studies should focus on understanding whether the effects observed in our experiments are dependent on its interaction with β-catenin[68] or other co-repressors or co-activators[69–71] or whether they may reflect the ability of *TCF7L2* to integrate signaling from other pathways, including TGF-β via *SMAD3*.[72]

Current treatment of aortic aneurysms involves surgical repair to reduce the risk of rupture, yet only a fraction of patients are eligible and those who are eligible are at high risk for post-surgery complications. Therapies for stabilization of aortic aneurysms have yet to prove efficacy in controlled clinical trials. Because of the involvement of this pathway in various diseases, present efforts in the drug development field are aimed at identifying inhibitors of the β-catenin-*TCF7L2* interactions[73] and the design of specific approaches targeting *TCF7L2* stability.[74] Our findings here highlight a potential path for *TCF7L2* as a target for intervention in individuals with TAA or for possible prevention in individuals at risk of TAA.

Data and code availability

TAA GWAS summary statistics from CHIP+MGI are available here: http://csg.sph.umich.edu/willer/public/TAA2021/. Analyses were performed by open-source software and cited in the material and methods.

Supplemental information

Supplemental information can be found online at https://doi.org/10.1016/j.ajhg.2021.06.016.

Acknowledgments

and Health Sciences, NTNU, Norwegian University of Science and Technology (NTNU), and Central Norway Regional Health Authority.

Web resources

DIAGRAM, https://diagram-consortium.org
ENCODE, https://www.encodeproject.org/
GTEx Portal, http://www.gtexportal.org/home/index.html
Promoter capture Hi-C, http://www.3div.kr/capture_hic

References

1. Hiratzka, L.F., Bakris, G.L., Beckman, J.A., Bersin, R.M., Carr, V.F., Casey, D.E., Jr., Eagle, K.A., Hermann, L.K., Isselbacher, E.M., Kazerooni, E.A., et al. (2010). 2010 ACCF/AHA/AATS/ACR/ASA/SCA/SCAI/SIR/STS/SVM guidelines for the diagnosis and management of patients with Thoracic Aortic Disease: a report of the American College of Cardiology Foundation/American Heart Association Task Force on Practice Guidelines, American Association for Thoracic Surgery, American College of Radiology, American Stroke Association, Society of Cardiovascular Anesthesiologists, Society for Cardiovascular Angiography and Interventions, Society of Interventional Radiology, Society of Thoracic Surgeons, and Society for Vascular Medicine. Circulation 121, e266–e369.

2. Pinard, A., Jones, G.T., and Milewicz, D.M. (2019). Genetics of Thoracic and Abdominal Aortic Diseases. Circ. Res. 124, 588–606.

3. Wolford, B.N., Hornsby, W.E., Guo, D., Zhou, W., Lin, M., Farhat, L., McNamara, J., Driscoll, A., Wu, X., Schmidt, E.M., et al. (2019). Clinical Implications of Identifying Pathogenic Variants in Individuals With Thoracic Aortic Dissection. Circ Genom Precis Med 12, e002476.

4. Renard, M., Francis, C., Ghosh, R., Scott, A.F., Witmer, P.D., Adès, L.C., Andelfinger, G.U., Arnaud, P., Boileau, C., Callewaert, B.L., et al. (2018). Clinical Validity of Genes for Heritable Thoracic Aortic Aneurysm and Dissection. J. Am. Coll. Cardiol. 72, 605–615.

5. Dietz, H.C., Cutting, G.R., Pyeritz, R.E., Maslen, C.L., Sakai, L.Y., Corson, G.M., Puffenberger, E.G., Hamosh, A., Nanthakumar, E.J., Curristin, S.M., et al. (1991). Marfan syndrome caused by a recurrent de novo missense mutation in the fibrillin gene. Nature 352, 337–339.

6. Loeys, B.L., Schwarze, U., Holm, T., Callewaert, B.L., Thomas, G.H., Pannu, H., De Backer, J.F., Oswald, G.L., Symoens, S., Manouvrier, S., et al. (2006). Aneurysm syndromes caused by mutations in the TGF-beta receptor. N. Engl. J. Med. 355, 788–798.

7. Rooprai, J., Boodhwani, M., Beauchesne, L., Chan, K.L., Dennie, C., Nagpal, S., Messika-Zeitoun, D., and Coutinho, T. (2019). Thoracic Aortic Aneurysm Growth in Bicuspid Aortic Valve Patients: Role of Aortic Stiffness and Pulsatile Hemodynamics. J. Am. Heart Assoc. 8, e010885.

8. LeMaire, S.A., McDonald, M.L., Guo, D.C., Russell, L., Miller, C.C., 3rd, Johnson, R.J., Bekheirnia, M.R., Franco, L.M., Nguyen, M., Pyeritz, R.E., et al. (2011). Genome-wide association study identifies a susceptibility locus for thoracic aortic aneurysms and aortic dissections spanning FBN1 at 15q21.1. Nat. Genet. 43, 996–1000.

9. Guo, D.C., Grove, M.L., Prakash, S.K., Eriksson, P., Hostetler, E.M., LeMaire, S.A., Body, S.C., Shalhub, S., Estrera, A.L., Safi, H.J., et al. (2016). Genetic Variants in LRP1 and ULK4 Are Associated with Acute Aortic Dissections. Am. J. Hum. Genet. 99, 762–769.

10. Fritsche, L.G., Gruber, S.B., Wu, Z., Schmidt, E.M., Zawistowski, M., Moser, S.E., Blanc, V.M., Brummett, C.M., Kheterpal, S., Abecasis, G.R., and Mukherjee, B. (2018). Association of Polygenic Risk Scores for Multiple Cancers in a Phenomewide Study: Results from The Michigan Genomics Initiative. Am. J. Hum. Genet. 102, 1048–1061.

11. Jun, G., Flickinger, M., Hetrick, K.N., Romm, J.M., Doheny, K.F., Abecasis, G.R., Boehnke, M., and Kang, H.M. (2012). Detecting and estimating contamination of human DNA samples in sequencing and array-based genotype data. Am. J. Hum. Genet. 91, 839–848.

12. Taliun, D., Chothani, S.P., Schönherr, S., Forer, L., Boehnke, M., Abecasis, G.R., and Wang, C. (2017). LASER server: ancestry tracing with genotypes or sequence reads. Bioinformatics 33, 2056–2058.

13. Manichaikul, A., Mychaleckyj, J.C., Rich, S.S., Daly, K., Sale, M., and Chen, W.M. (2010). Robust relationship inference in genome-wide association studies. Bioinformatics 26, 2867–2873.

14. McCarthy, S., Das, S., Kretzschmar, W., Delaneau, O., Wood, A.R., Teumer, A., Kang, H.M., Fuchsberger, C., Danecek, P., Sharp, K., et al. (2016). A reference panel of 64,976 haplotypes for genotype imputation. Nat. Genet. 48, 1279–1283.

15. Das, S., Forer, L., Schönherr, S., Sidore, C., Locke, A.E., Kwong, A., Vrieze, S.I., Chew, E.Y., Levy, S., McGue, M., et al. (2016). Next-generation genotype imputation service and methods. Nat. Genet. 48, 1284–1287.

16. Yang, B., Zhou, W., Jiao, J., Nielsen, J.B., Mathis, M.R., Heydarpour, M., Lettre, G., Folkersen, L., Prakash, S., Schurmann, C., et al. (2017). Protein-altering and regulatory genetic variants near GATA4 implicated in bicuspid aortic valve. Nat. Commun. 8, 15481.

17. Pasta, S., Rinaudo, A., Luca, A., Pilato, M., Scardulla, C., Gleason, T.G., and Vorp, D.A. (2013). Difference in hemodynamic and wall stress of ascending thoracic aortic aneurysms with bicuspid and tricuspid aortic valve. J. Biomech. 46, 1729–1738.

18. Zhou, W., Nielsen, J.B., Fritsche, L.G., Dey, R., Gabrielsen, M.E., Wolford, B.N., LeFaive, J., VandeHaar, P., Gagliano, S.A., Gifford, A., et al. (2018). Efficiently controlling for case-control imbalance and sample relatedness in large-scale genetic association studies. Nat. Genet. 50, 1335–1341.

19. Hunter-Zinck, H., Shi, Y., Li, M., Gorman, B.R., Ji, S.G., Sun, N., Webster, T., Liem, A., Hsieh, P., Deviveni, P., et al. (2020). Genotyping Array Design and Data Quality Control in the Million Veteran Program. Am. J. Hum. Genet. 106, 535–548.

20. Fang, H., Hui, Q., Lynch, J., Honerlaw, J., Assimes, T.L., Huang, J., Vujkovic, M., Damrauer, S.M., Pyarajan, S., Gaziano, J.M., et al. (2019). Harmonizing Genetic Ancestry and Self-identified Race/Ethnicity in Genome-wide Association Studies. Am. J. Hum. Genet. 105, 763–772.

21. Krokstad, S., Langhammer, A., Hveem, K., Holmen, T.L., Midthjell, K., Stene, T.R., Bratberg, G., Heggland, J., and Holmen, J. (2013). Cohort Profile: the HUNT Study, Norway. Int. J. Epidemiol. *42*, 968–977.

22. Nielsen, J.B., Thorolfsdottir, R.B., Fritsche, L.G., Zhou, W., Skov, M.W., Graham, S.E., Herron, T.J., McCarthy, S., Schmidt, E.M., Sveinbjornsson, G., et al. (2018). Biobank-driven genomic discovery yields new insight into atrial fibrillation biology. Nat. Genet. *50*, 1234–1239.

23. Sudlow, C., Gallacher, J., Allen, N., Beral, V., Burton, P., Danesh, J., Downey, P., Elliott, P., Green, J., Landray, M., et al. (2015). UK biobank: an open access resource for identifying the causes of a wide range of complex diseases of middle and old age. PLoS Med. *12*, e1001779.

24. Willer, C.J., Li, Y., and Abecasis, G.R. (2010). METAL: fast and efficient meta-analysis of genomewide association scans. Bioinformatics *26*, 2190–2191.

25. Jung, I., Schmitt, A., Diao, Y., Lee, A.J., Liu, T., Yang, D., Tan, C., Eom, J., Chan, M., Chee, S., et al. (2019). A compendium of promoter-centered long-range chromatin interactions in the human genome. Nat. Genet. *51*, 1442–1449.

26. Yang, J., Lee, S.H., Goddard, M.E., and Visscher, P.M. (2011). GCTA: a tool for genome-wide complex trait analysis. Am. J. Hum. Genet. *88*, 76–82.

27. Giambartolomei, C., Vukcevic, D., Schadt, E.E., Franke, L., Hingorani, A.D., Wallace, C., and Plagnol, V. (2014). Bayesian test for colocalisation between pairs of genetic association studies using summary statistics. PLoS Genet. *10*, e1004383.

28. Barbeira, A.N., Dickinson, S.P., Bonazzola, R., Zheng, J., Wheeler, H.E., Torres, J.M., Torstenson, E.S., Shah, K.P., Garcia, T., Edwards, T.L., et al. (2018). Exploring the phenotypic consequences of tissue specific gene expression variation inferred from GWAS summary statistics. Nat. Commun. *9*, 1825.

29. GTEx Consortium (2020). The GTEx Consortium atlas of genetic regulatory effects across human tissues. Science *369*, 1318–1330.

30. Benner, C., Spencer, C.C., Havulinna, A.S., Salomaa, V., Ripatti, S., and Pirinen, M. (2016). FINEMAP: efficient variable selection using summary data from genome-wide association studies. Bioinformatics *32*, 1493–1501.

31. Purcell, S., Neale, B., Todd-Brown, K., Thomas, L., Ferreira, M.A., Bender, D., Maller, J., Sklar, P., de Bakker, P.I., Daly, M.J., and Sham, P.C. (2007). PLINK: a tool set for whole-genome association and population-based linkage analyses. Am. J. Hum. Genet. *81*, 559–575.

32. Boyle, A.P., Hong, E.L., Hariharan, M., Cheng, Y., Schaub, M.A., Kasowski, M., Karczewski, K.J., Park, J., Hitz, B.C., Weng, S., et al. (2012). Annotation of functional variation in personal genomes using RegulomeDB. Genome Res. *22*, 1790–1797.

33. Snyder, M.P., Gingeras, T.R., Moore, J.E., Weng, Z., Gerstein, M.B., Ren, B., Hardison, R.C., Stamatoyannopoulos, J.A., Graveley, B.R., Feingold, E.A., et al. (2020). Perspectives on ENCODE. Nature *583*, 693–698.

34. Bulik-Sullivan, B.K., Loh, P.R., Finucane, H.K., Ripke, S., Yang, J., Patterson, N., Daly, M.J., Price, A.L., Neale, B.M.; and Schizophrenia Working Group of the Psychiatric Genomics Consortium (2015). LD Score regression distinguishes confounding from polygenicity in genome-wide association studies. Nat. Genet. *47*, 291–295.

35. Zheng, J., Erzurumluoglu, A.M., Elsworth, B.L., Kemp, J.P., Howe, L., Haycock, P.C., Hemani, G., Tansey, K., Laurin, C., Pourcain, B.S., et al. (2017). LD Hub: a centralized database and web interface to perform LD score regression that maximizes the potential of summary level GWAS data for SNP heritability and genetic correlation analysis. Bioinformatics *33*, 272–279.

36. Tetsu, O., and McCormick, F. (1999). Beta-catenin regulates expression of cyclin D1 in colon carcinoma cells. Nature *398*, 422–426.

37. Lu, H., Sun, J., Liang, W., Chang, Z., Rom, O., Zhao, Y., Zhao, G., Xiong, W., Wang, H., Zhu, T., et al. (2020). Cyclodextrin Prevents Abdominal Aortic Aneurysm via Activation of Vascular Smooth Muscle Cell Transcription Factor EB. Circulation *142*, 483–498.

38. Kälsch, H., Lehmann, N., Möhlenkamp, S., Becker, A., Moebus, S., Schmermund, A., Stang, A., Mahabadi, A.A., Mann, K., Jöckel, K.H., et al. (2013). Body-surface adjusted aortic reference diameters for improved identification of patients with thoracic aortic aneurysms: results from the population-based Heinz Nixdorf Recall study. Int. J. Cardiol. *163*, 72–78.

39. Klarin, D., Verma, S.S., Judy, R., Dikilitas, O., Wolford, B.N., Paranjpe, I., Levin, M.G., Pan, C., Tcheandjieu, C., Spin, J.M., et al. (2020). Genetic Architecture of Abdominal Aortic Aneurysm in the Million Veteran Program. Circulation *142*, 1633–1646.

40. Bakker, M.K., van der Spek, R.A.A., van Rheenen, W., Morel, S., Bourcier, R., Hostettler, I.C., Alg, V.S., van Eijk, K.R., Koido, M., Akiyama, M., et al. (2020). Genome-wide association study of intracranial aneurysms identifies 17 risk loci and genetic overlap with clinical risk factors. Nat. Genet. *52*, 1303–1313.

41. Grant, S.F., Thorleifsson, G., Reynisdottir, I., Benediktsson, R., Manolescu, A., Sainz, J., Helgason, A., Stefansson, H., Emilsson, V., Helgadottir, A., et al. (2006). Variant of transcription factor 7-like 2 (TCF7L2) gene confers risk of type 2 diabetes. Nat. Genet. *38*, 320–323.

42. Gloyn, A.L., Braun, M., and Rorsman, P. (2009). Type 2 diabetes susceptibility gene TCF7L2 and its role in beta-cell function. Diabetes *58*, 800–802.

43. Mahajan, A., Taliun, D., Thurner, M., Robertson, N.R., Torres, J.M., Rayner, N.W., Payne, A.J., Steinthorsdottir, V., Scott, R.A., Grarup, N., et al. (2018). Fine-mapping type 2 diabetes loci to single-variant resolution using high-density imputation and islet-specific epigenome maps. Nat. Genet. *50*, 1505–1513.

44. Hormozdiari, F., Kostem, E., Kang, E.Y., Pasaniuc, B., and Eskin, E. (2014). Identifying causal variants at loci with multiple signals of association. Genetics *198*, 497–508.

45. He, R., Guo, D.C., Estrera, A.L., Safi, H.J., Huynh, T.T., Yin, Z., Cao, S.N., Lin, J., Kurian, T., Buja, L.M., et al. (2006). Characterization of the inflammatory and apoptotic cells in the aortas of patients with ascending thoracic aortic aneurysms and dissections. J. Thorac. Cardiovasc. Surg. *131*, 671–678.

46. Durdu, S., Deniz, G.C., Balci, D., Zaim, C., Dogan, A., Can, A., Akcali, K.C., and Akar, A.R. (2012). Apoptotic vascular smooth muscle cell depletion via BCL2 family of proteins in human ascending aortic aneurysm and dissection. Cardiovasc. Ther. *30*, 308–316.

47. Srivastava, R., Rolyan, H., Xie, Y., Li, N., Bhat, N., Hong, L., Esteghamat, F., Adeniran, A., Geirsson, A., Zhang, J., et al. (2019). TCF7L2 (Transcription Factor 7-Like 2) Regulation of GATA6 (GATA-Binding Protein 6)-Dependent and -Independent Vascular Smooth Muscle Cell Plasticity and Intimal Hyperplasia. Arterioscler. Thromb. Vasc. Biol. *39*, 250–262.

48. Srivastava, R., Zhang, J., Go, G.W., Narayanan, A., Nottoli, T.P., and Mani, A. (2015). Impaired LRP6-TCF7L2 Activity

Enhances Smooth Muscle Cell Plasticity and Causes Coronary Artery Disease. Cell Rep. *13*, 746–759.

49. Wang, X., Adhikari, N., Li, Q., and Hall, J.L. (2004). LDL receptor-related protein LRP6 regulates proliferation and survival through the Wnt cascade in vascular smooth muscle cells. Am. J. Physiol. Heart Circ. Physiol. *287*, H2376–H2383.

50. Liu, X., Huang, Y., Zhang, Y., Li, X., Liu, C., Huang, S., Xu, D., Wu, Y., and Liu, X. (2016). T-cell factor (TCF/LEF1) binding elements (TBEs) of FasL (Fas ligand or CD95 ligand) bind and cluster Fas (CD95) and form complexes with the TCF-4 and b-catenin transcription factors in vitro and in vivo which result in triggering cell death and/or cell activation. Cell. Mol. Neurobiol. *36*, 1001–1013.

51. Ma, B., Zhong, L., van Blitterswijk, C.A., Post, J.N., and Karperien, M. (2013). T cell factor 4 is a pro-catabolic and apoptotic factor in human articular chondrocytes by potentiating nuclear factor κB signaling. J. Biol. Chem. *288*, 17552–17558.

52. Li, H., Ma, Y., Chen, B., and Shi, J. (2018). miR-182 enhances acute kidney injury by promoting apoptosis involving the targeting and regulation of TCF7L2/Wnt/β-catenins pathway. Eur. J. Pharmacol. *831*, 20–27.

53. Zhou, Y., Zhang, E., Berggreen, C., Jing, X., Osmark, P., Lang, S., Cilio, C.M., Göransson, O., Groop, L., Renström, E., and Hansson, O. (2012). Survival of pancreatic beta cells is partly controlled by a TCF7L2-p53-p53INP1-dependent pathway. Hum. Mol. Genet. *21*, 196–207.

54. Henderson, E.L., Geng, Y.J., Sukhova, G.K., Whittemore, A.D., Knox, J., and Libby, P. (1999). Death of smooth muscle cells and expression of mediators of apoptosis by T lymphocytes in human abdominal aortic aneurysms. Circulation *99*, 96–104.

55. Viñuela, A., Varshney, A., van de Bunt, M., Prasad, R.B., Asplund, O., Bennett, A., Boehnke, M., Brown, A.A., Erdos, M.R., Fadista, J., et al. (2020). Genetic variant effects on gene expression in human pancreatic islets and their implications for T2D. Nat. Commun. *11*, 4912.

56. Patel, K., Zafar, M.A., Ziganshin, B.A., and Elefteriades, J.A. (2018). Diabetes Mellitus: Is It Protective against Aneurysm? A Narrative Review. Cardiology *141*, 107–122.

57. Takagi, H., Umemoto, T.; and ALICE (All-Literature Investigation of Cardiovascular Evidence) Group (2017). Negative Association of Diabetes With Thoracic Aortic Dissection and Aneurysm. Angiology *68*, 216–224.

58. Raffort, J., Lareyre, F., Clément, M., Hassen-Khodja, R., Chinetti, G., and Mallat, Z. (2018). Diabetes and aortic aneurysm: current state of the art. Cardiovasc. Res. *114*, 1702–1713.

59. Yi, F., Brubaker, P.L., and Jin, T. (2005). TCF-4 mediates cell type-specific regulation of proglucagon gene expression by beta-catenin and glycogen synthase kinase-3beta. J. Biol. Chem. *280*, 1457–1464.

60. Komiya, Y., and Habas, R. (2008). Wnt signal transduction pathways. Organogenesis *4*, 68–75.

61. Ng, L.F., Kaur, P., Bunnag, N., Suresh, J., Sung, I.C.H., Tan, Q.H., Gruber, J., and Tolwinski, N.S. (2019). WNT Signaling in Disease. Cells *8*, E826.

62. Facchinello, N., Tarifeño-Saldivia, E., Grisan, E., Schiavone, M., Peron, M., Mongera, A., Ek, O., Schmitner, N., Meyer, D., Peers, B., et al. (2017). Tcf7l2 plays pleiotropic roles in the control of glucose homeostasis, pancreas morphology, vascularization and regeneration. Sci. Rep. *7*, 9605.

63. Wang, S., Huang, H., Xiang, H., Gu, B., Li, W., Chen, L., and Zhang, M. (2019). Wnt Signaling Modulates Routes of Retinoic Acid-Induced Differentiation of Embryonic Stem Cells. Stem Cells Dev. *28*, 1334–1345.

64. Corada, M., Nyqvist, D., Orsenigo, F., Caprini, A., Giampietro, C., Taketo, M.M., Iruela-Arispe, M.L., Adams, R.H., and Dejana, E. (2010). The Wnt/beta-catenin pathway modulates vascular remodeling and specification by upregulating Dll4/Notch signaling. Dev. Cell *18*, 938–949.

65. Wang, X., Xiao, Y., Mou, Y., Zhao, Y., Blankesteijn, W.M., and Hall, J.L. (2002). A role for the beta-catenin/T-cell factor signaling cascade in vascular remodeling. Circ. Res. *90*, 340–347.

66. Krishna, S.M., Seto, S.W., Jose, R.J., Li, J., Morton, S.K., Biros, E., Wang, Y., Nsengiyumva, V., Lindeman, J.H., Loots, G.G., et al. (2017). Wnt Signaling Pathway Inhibitor Sclerostin Inhibits Angiotensin II-Induced Aortic Aneurysm and Atherosclerosis. Arterioscler. Thromb. Vasc. Biol. *37*, 553–566.

67. Kostina, A., Bjork, H., Ignatieva, E., Irtyuga, O., Uspensky, V., Semenova, D., Maleki, S., Tomilin, A., Moiseeva, O., Franco-Cereceda, A., et al. (2018). Notch, BMP and WNT/β-catenin network is impaired in endothelial cells of the patients with thoracic aortic aneurysm. Atheroscler. Suppl. *35*, e6–e13.

68. Graham, T.A., Ferkey, D.M., Mao, F., Kimelman, D., and Xu, W. (2001). Tcf4 can specifically recognize beta-catenin using alternative conformations. Nat. Struct. Biol. *8*, 1048–1052.

69. Valenta, T., Lukas, J., and Korinek, V. (2003). HMG box transcription factor TCF-4's interaction with CtBP1 controls the expression of the Wnt target Axin2/Conductin in human embryonic kidney cells. Nucleic Acids Res. *31*, 2369–2380.

70. Brantjes, H., Roose, J., van De Wetering, M., and Clevers, H. (2001). All Tcf HMG box transcription factors interact with Groucho-related co-repressors. Nucleic Acids Res. *29*, 1410–1419.

71. Hecht, A., and Stemmler, M.P. (2003). Identification of a promoter-specific transcriptional activation domain at the C terminus of the Wnt effector protein T-cell factor 4. J. Biol. Chem. *278*, 3776–3785.

72. Labbé, E., Letamendia, A., and Attisano, L. (2000). Association of Smads with lymphoid enhancer binding factor 1/T cell-specific factor mediates cooperative signaling by the transforming growth factor-beta and wnt pathways. Proc. Natl. Acad. Sci. USA *97*, 8358–8363.

73. Tian, W., Han, X., Yan, M., Xu, Y., Duggineni, S., Lin, N., Luo, G., Li, Y.M., Han, X., Huang, Z., and An, J. (2012). Structure-based discovery of a novel inhibitor targeting the β-catenin/Tcf4 interaction. Biochemistry *51*, 724–731.

74. Zhang, H., Rong, X., Wang, C., Liu, Y., Lu, L., Li, Y., Zhao, C., and Zhou, J. (2020). VBP1 modulates Wnt/β-catenin signaling by mediating the stability of the transcription factors TCF/LEFs. J. Biol. Chem. *295*, 16826–16839.